TSINGHUA SCIENCE AND TECHNOLOGY
ISSN 1007-0214 12/19 pp577-584
Volume 12, Number 5, October 2007

Reference Trajectory Generation for 3-Dimensional Walking of a Humanoid Robot*

TANG Zhe (汤 哲), SUN Zengqi (孙增圻)**,
ZHOU Changjiu (周长久)†, HU Lingyun (胡凌云)

Department of Computer Science and Technology, Tsinghua University, Beijing 100084, China;
† School of Electrical and Electronic Engineering, Singapore Polytechnic, 500 Dover Road, Singapore 139651, Singapore

Abstract: Humanoid walking planning is a complicated task because of the high number of degrees of freedom (DOFs) and the variable mechanical structure during walking. In this paper, a planning method for 3-dimensional (3-D) walking movements was developed based on a model of a typical humanoid robot with 12 DOFs on the lower body. The planning process includes trajectory generation for the hip, ankle, and knee joints in the Cartesian space. The balance of the robot was ensured by adjusting the hip motion. The angles for each DOF were obtained from 3-D kinematics calculation. The calculation gave reference trajectories of all the DOFs on the humanoid robot which were used to control the real robot. The simulation results show that the method is effective.

Key words: humanoid robots; walking planning; trajectory generation; robot kinematics

Introduction

Humanoid robot research has been a popular research topic in the robotics field for decades. Humanoid robots possess higher mobility and flexibility than conventional wheeled robots. Robots have to be able to adapt to complicated environments, such as rugged terrain, sloped surfaces, and steep stairs. The humanoid robot control systems need to provide high performance mobility, behavioural robustness, behavioural complexity, control of high degrees of freedom (DOFs) systems, etc[1].

Much work has been devoted to the synthesis of realistic walking gaits for humanoid robots. Reference trajectories are needed for each DOF to control waking of a real humanoid robot, so the design of reference trajectories for walking gait is important. Vukobratovic et al.[2] adopted a two-stage control synthesis approach. In the first stage, the control synthesis ensures the system's stability in the absence of any disturbance along the exact reference trajectories calculated in advance. In the second stage, external perturbations are added to the system. The nominal gait is realized by assistance from an additional control force. Shih[3, 4] proposed a gait synthesis for ascending and descending stairs for his 7-DOF biped. The efficiency of the gait synthesis was supported by the biped implementation. However, his method was only applicable to his specific humanoid with variable length legs and translatable balance weight in the body. Miyazaki and Arimoto[5] divided biped locomotion into a slow mode and a fast mode. Joint motion trajectories were obtained in the two modes. They used the inverted pendulum model to approximate the biped global locomotion. Their control algorithm was verified by computer simulations. Chevallerau and Aoustin[6] gave a method to generate cyclic joint reference trajectories for walking and running of humanoids.

The optimization objectives of the gait included the

Received: 2005-04-22

* Supported by the National Natural Science Foundation of China (Nos. 90405017 and 60604010)

** To whom correspondence should be addressed.
E-mail: szq-dcs@tsinghua.edu.cn; Tel: 86-10-62788939

maximum advance velocity, minimum torque, and minimal energy. Furusho and Sano[7] achieved smooth 3-dimensional (3-D) walking with a sensor-based control on a biped with nine links. They considered the motion in the lateral plane as a regulator problem with two equilibrium states. In the sagittal plane, where the walking control was based on the body speed in the forward direction, they made the body movement close to the desired smooth speed by controlling the ankle torque of the support leg. The sole and ankle driving actuators underwent a force/torque feedback control based on the sensor information. An inverted pendulum mode was adopted for the robot dynamic model. Mita et al.[8] used a linear optimal state feedback regulator to control a seven-link biped. Their work proved the usefulness of typical modern control theory for studies on biped locomotion. Miura and Shimoyama[9] approximated the biped motion of the single support phase as an inverted pendulum, and gave a trajectory planning and stability analysis. Their methods were implemented on their two biped robots. Zheng and Shen[10] developed a biped robot, SD-2, which could climb sloping surfaces using static stabilization criteria. A force sensor underneath the foot was able to detect the transition of the supporting terrain from a flat floor to a sloping surface of up to 10°. They were the first to propose a biped walking algorithm on a sloped surface. Huang et al.[11] presented a practical method for humanoid robot trajectory planning using the third-order spline interpolation method. However, their walking planning was limited to humanoid motion in the sagittal plane.

Most current humanoid motion gait synthesis methods are based on a simplified model, such as inverted pendulum model[5] or decomposition of the motion into two independent planes[6,11], which leads to difficult implementation in real robots. This paper describes a walking gait synthesis method based on a 3-D model of a humanoid robot. The method uses a 12-DOF model of the humanoid robot, a typical lower body structure. The novelty of this work lies in the adoption of the 3-D model for the walking planning. The reference trajectories of the 12 DOFs generated by the method are accurate, because there is no kinematic simplifications involved. As a result, real robots can be controlled by using these reference trajectories. Unlike the work of Vukobratovic et al.[2] or Miyazaki and Arimoto[5], this work focuses on high level path planning for humanoid walking gait synthesis. This paper extends the walking planning method from 2-D to 3-D. Robot motions in both the sagittal and frontal planes are taken into consideration. In addition, the method is valid for a typical class of humanoid robots with 12 DOFs on the lower body, not just for a specific robot.

1 Humanoid Robot Structure

The humanoid robot Robo-Erectus (Fig. 1) is used in our experiments. The robot was developed by the Advanced Robotics and Intelligent Control Centre (ARICC) at Singapore Polytechnic. The current research considers only the lower body for robot balance. Each leg has six DOFs with three DOFs at the hip, one at the knee, and two at the ankle. The robot is 50 cm tall and weighs 4 kg. The robot sensor system consists of a vision system, range sensors, electric compass, gyros, and force sensors.

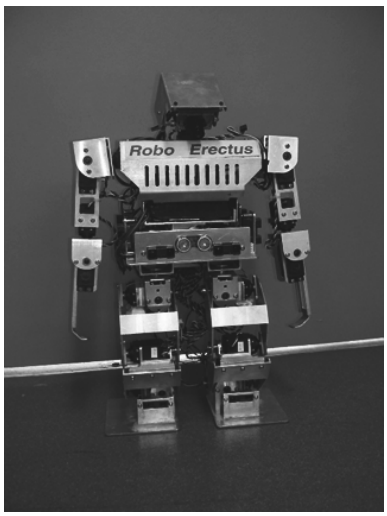

Fig 1 Robo-Erectus

The robot control structure is diagrammed in Fig. 2. The hierarchical control structure is decomposed into an offline level, a high level, a middle level, and a low level. The simulation software generates many kinds of humanoid motions such as walking at different speeds, kicking, and turning. These motions are represented as sets of trajectories for each DOF, which are used as reference trajectories for the robot control. The walking planning is accomplished in this level. Because this process is done offline, time consuming intelligent techniques, such as GAs, neural networks, and machine learning can be implemented to optimize the

humanoid motion planning. However, because it is impossible to simulate the complete dynamics and kinematics of the robot, the motion generated offline may need to be revised through actual running on a real robot. The high level control does path planning, which generates a path from a start to a goal based on sensor information. To follow the path generated by the high level control, the robot needs to accomplish different kinds of motion, walking, turning, sometimes walking faster and sometimes more slowly. These decisions are made by the middle level control. The low level control is closely related to the robot hardware, which tries to minimize the error between the reference angles and the actual angles of the robot DOFs.

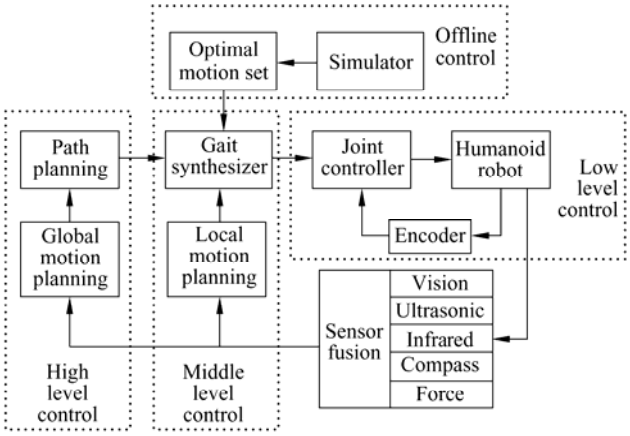

Fig. 2 Schematic diagram of the hierarchical control system

Simulation software was developed for humanoid motion planning based on the Robo-Erectus, which can generate trajectories for each robot DOF in both Cartesian space and Joint space. The torque on every DOF and zero moment point (ZMP) is also obtained. These two kinds of information are used to evaluate the robot motion performance.

2 Humanoid Robot Dynamics

The mechanical structural model of the humanoid robot varies during walking[2]. In the single support phase, the humanoid robot can be analyzed as a mechanism composed of several open kinematic chains. In the double support phase the robot can be analyzed as closed kinematic chains. Therefore, the dynamic equations for the two walking phases differ. The single support phase can be described by

$$\boldsymbol{\tau} = \boldsymbol{D}(\boldsymbol{q})\ddot{\boldsymbol{q}} + \boldsymbol{C}(\boldsymbol{q},\dot{\boldsymbol{q}}) + \boldsymbol{g}(\boldsymbol{q}) \quad (1)$$

where $\boldsymbol{q}$ is the $n\times 1$ vector of the generalized joint displacements, $\boldsymbol{\tau}$ is the $n\times 1$ vector of the applied generalized forces, $\boldsymbol{D}(\boldsymbol{q})$ is the $n\times n$ mass matrix, $\boldsymbol{C}(\boldsymbol{q},\dot{\boldsymbol{q}})$ is the $n\times 1$ vector of the centrifugal and Coriolis terms, and $\boldsymbol{g}(\boldsymbol{q})$ is the $n\times 1$ vector of the gravity terms.

The dynamics of humanoid robots during the double support phase were studied by Mitobe et al.[12]

$$\boldsymbol{\tau} = \boldsymbol{D}(\boldsymbol{q})\boldsymbol{F}(\ddot{\boldsymbol{q}}_{\mathrm{d}} - \boldsymbol{K}_{\mathrm{pd}}\dot{\boldsymbol{q}}_{\mathrm{e}} - \boldsymbol{K}_{\mathrm{pp}}\boldsymbol{q}_{\mathrm{e}}) + \boldsymbol{C}^{\mathrm{T}}\lambda_u + \boldsymbol{D}(\boldsymbol{q})\phi + \boldsymbol{h} \quad (2)$$

where $\ddot{\boldsymbol{q}}_{\mathrm{d}}$ is the desired robot trajectories, $\boldsymbol{q}_{\mathrm{e}}$ is the error between the desired trajectory and real trajectory, λ_u represents the constraint forces, $\boldsymbol{C}^{\mathrm{T}}\lambda_u$ represents the torques at each joint due to the constraints, $\boldsymbol{K}_{\mathrm{pp}}$ and $\boldsymbol{K}_{\mathrm{pd}}$ are diagonal matrices of the positive gains ϕ is the inertial force, and $\boldsymbol{h}$ is the gravitational, centripetal, and Coriolis term.

3 Kinematic Constraints

A humanoid robot with 12 DOFs has many possible gaits in 3-D space. A feasible walking gait needs to identify the constraints between these DOFs (DOFs definitions given in Fig. 3).

(1) DOFs 2, 3, and 4 constitute a plane S_1. Plane S_2 passes through DOF 1 and is parallel to the foot print plane. The intersection between S_1 and S_2 is line L_1.

(2) The angle of DOF 1 is the plane angle between S_1 and S_2.

(3) DOF 5 and the hip link constitute plane S_3. The angle of DOF 5 is the angle between S_1 and S_3.

(4) DOF 5 and DOF 6 constitute plane S_4. The angle of DOF 6 is the angle between S_1 and S_4

(5) The angles of DOFs 2, 3, and 4 form a triangular relationship in plane S_1.

The walking gait planning assumes that S_2 is parallel to S_3 and the ground.

With these 3-D kinematic constraints, the angles for each DOF are calculated as follows.

(1) DOF 1: the plane angle between line L_1 and plane S_2;

(2) DOFs 2, 3, and 4: triangular relationship in plane S_1;

(3) DOF 5: angle between S_1 and S_3;

(4) DOF 6: angle between S_1 and S_4.

The angle between the two planes can be calculated by the following equations.

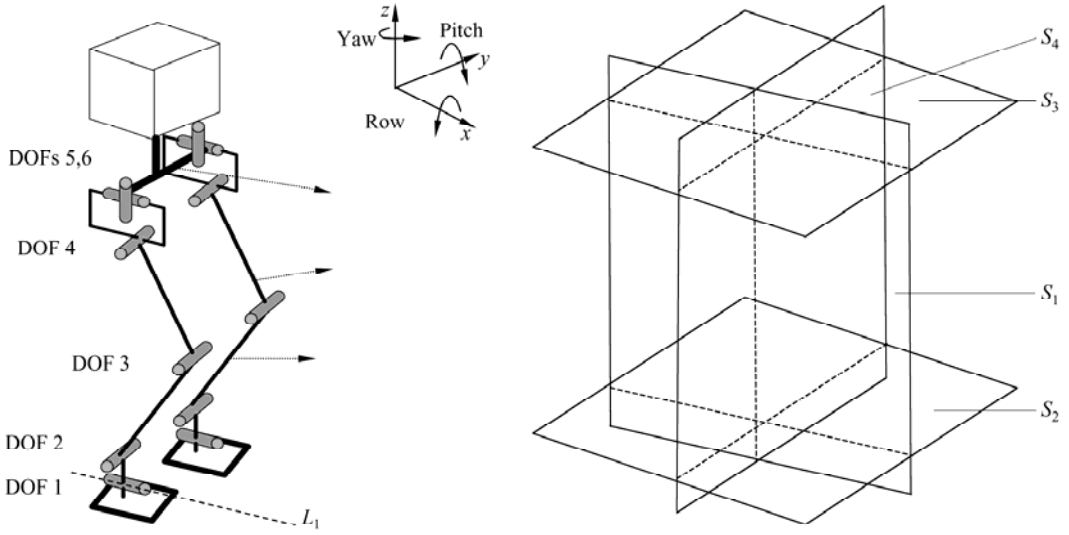

(a) Schematic of the lower body of the humanoid robot (b) Planes defined by the DOFs of the humanoid lower body

Fig. 3 The robot motion in the three planes

$$P_1: \quad A_1x + B_1y + C_1z + D_1 = 0,$$
$$P_2: \quad A_2x + B_2y + C_2z + D_2 = 0,$$
$$\varphi = \arccos\left(\frac{A_1A_2 + B_1B_2 + C_1C_2}{\sqrt{A_1A_1 + B_1B_1 + C_1C_1}\sqrt{A_2A_2 + B_2B_2 + C_2C_2}}\right) \quad (3)$$

where P_1 and P_2 are two planes.

4 Planning of Humanoid 3-D Walking

The humanoid robot movements require the trajectories of all joints. The trajectories should have first-order and second-order derivative continuity. The first order derivative continuity guarantees smoothness of the joint velocities, while the second order continuity guarantees smoothness of the acceleration or torque on the joints.

4.1 Ankle joint trajectory generation

Walking planning consists of trajectory generation for the ankle, hip, and knee in the Cartesian space. Reference trajectories in the joint space are obtained with 3-D kinematic constraints. The ankle joint trajectories are defined by the step length (L_{st}), walking cycle (T_c), double support time (T_d), and maximum swing height of the swing leg (H_{sw}). A third-order spline function is used to generate ankle joint trajectories. The ankle joint trajectory is defined once the foot trajectory is generated, which is given by the footstep planning[13] to follow a global path generated by the humanoid navigation system.

A typical walking cycle is given in Fig. 4. The walking cycle starts from the k-th step, where $kT_c + T_m$ corresponds to the point when the foot of the swing leg reaches its highest point, where the swing height is H_{ao}, the length relative to the support foot is L_{ao}. Figure 3 shows the robot motion in the three planes. The motion in the transverse plane gives the desired robot ZMP trajectory.

4.2 Hip joint trajectory generation

The mass distribution of the humanoid robot is mainly in the upper body. The hip motion mainly determines the trajectory of the center of gravity (COG) or the ZMP of the robot. The humanoid model has a left hip joint and right hip joint with a hip link between two hip joints. The center of the hip link is the pelvis. The pelvis trajectory is adjusted so that the ZMP is always kept in the foot support area.

The planning method assumes that the hip height is constant during walking. The objective of the pelvis trajectory is trying to follow the desired ZMP trajectory with ZMP in the foot support area. The hip link is parallel to the line determined by the two feet's projection in the x-y plane.

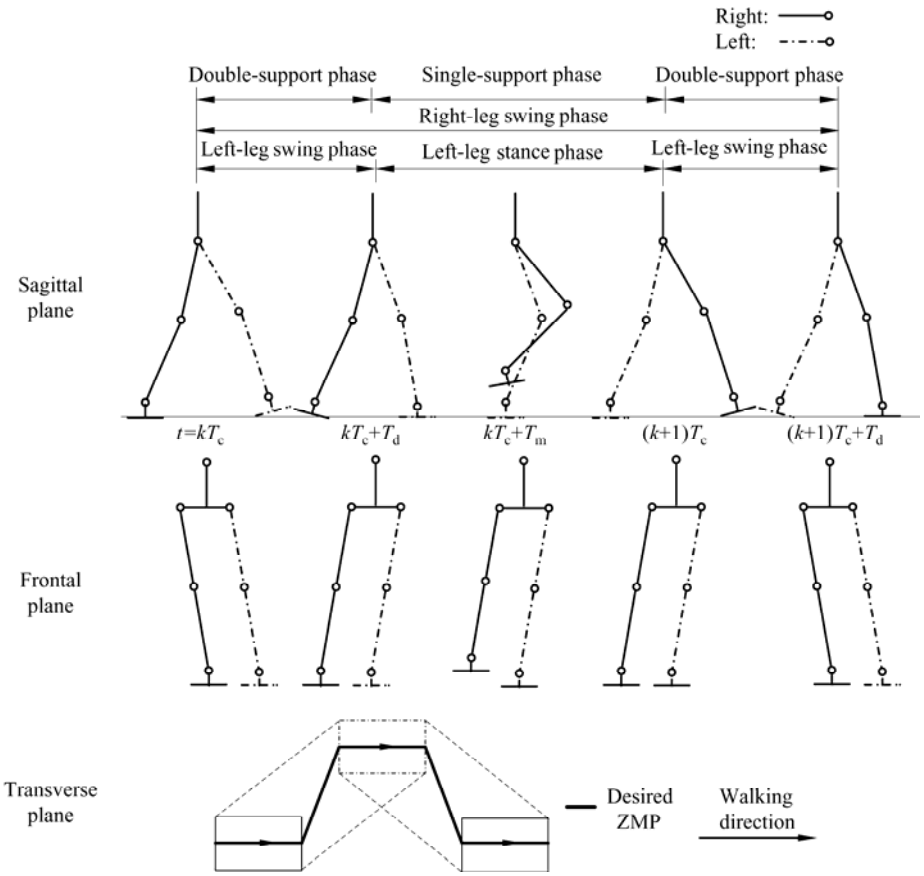

Fig. 4 Walking cycle

As shown in Fig. 5, Line $p_1p_2p_3p_4$ is the pelvis trajectory projection in the *x*-*y* plane. The adjustment of L_p makes sure that the ZMP of the robot is always in the support area. *A*, *B*, and *C* are the centers of the foot support areas. During the double support phase, the pelvis moves from p_1 to p_2. During the left-leg support phase, the pelvis moves from p_2 to p_3. During the second double support phase, the pelvis moves from p_3 to p_4. The two hip joint trajectories can then be obtained from these constraints.

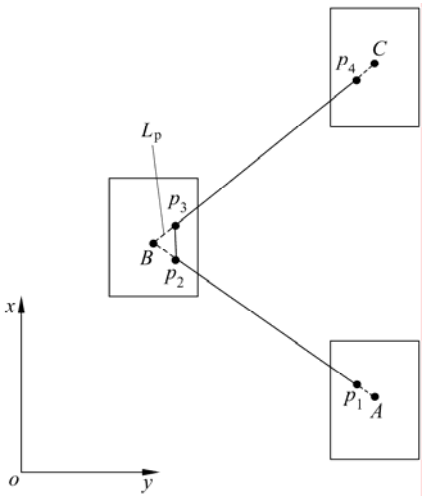

Fig. 5 Pelvis trajectory

4.3 Knee joint trajectory generation

After the foot trajectories and hip trajectories have been generated, the next step is to get the knee trajectories. Once the hip and ankle joint trajectories are given, the knee joint trajectories are defined by the robot kinematic constraints. The two knee trajectories can be obtained by solving

$$\frac{x-x_k}{x_h-x_k}=\frac{y-y_k}{y_h-y_k} \tag{4}$$

$$\frac{x-x_k}{x_h-x_k}=\frac{z-z_k}{z_h-z_k} \tag{5}$$

$$z=z_a \tag{6}$$

$$(x_h-x_k)^2+(y_h-y_k)^2+(z_h-z_k)^2=L_{th}{}^2 \tag{7}$$

$$(x_a-x_k)^2+(y_a-y_k)^2+(z_a-z_k)^2=L_{sh}{}^2 \tag{8}$$

$$x-x_a=(y-y_a)\tan\ \beta \tag{9}$$

where the unknowns are (x, y, z) which is the point where the line from DOF 4 to DOF 5 intersects line L_1. The (x_k, y_k, z_k) is the knee position. (x_h, y_h, z_h) is the hip position and (x_a, y_a, z_a) is the ankle position. Foot walking direction, β shown in Fig. 6 is obtained from the foot position. L_{th} and L_{sh} are the robot link parameters shown in Fig. 3.

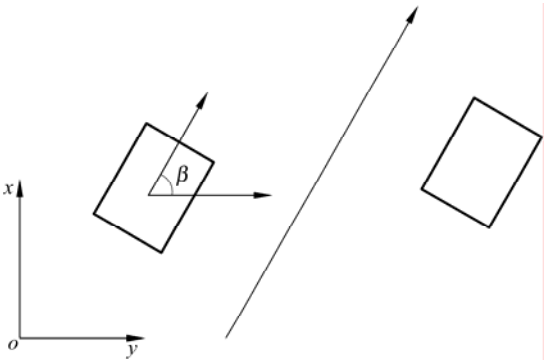

Fig. 6 Robot walking direction

Equations (4)-(9) are the humanoid kinematic constraints in 3-D space. Under the constraint 1, planes S_1 and S_2 always intersect on the line L_1. Therefore L_1 and the line from DOF 4 to DOF 5 must intersect at (x, y, z). Equations (4)-(6) represent the intersection point of the two lines. Equations (7) and (8) are the kinematic constraints and Eq. (9) is the relation between the walking direction and line L_1.

5 Simulation Results

The simulation software was developed from an earlier platform[14]. OpenGL was integrated to give a 3-D display of the humanoid robot. The software generates joint trajectories for each DOF of the humanoid robots. The reference trajectories of humanoid walking have been implemented on a real robot[15] to verify the effectiveness of the method.

The walking direction β was set as 60°, the double support time T_d was 0.2 s, the time of the maximum leg swing height T_m was 0.6 s, the walking cycle period T_c was 1 s, the step length L_{st} was 5 cm, and the leg maximum swing height H_{sm} was 1.5 cm.

The 12 reference trajectories for two walking cycles are shown in Figs. 7-10. These 12 reference trajectories were used to control the 12 DOFs of the real robot. The ZMP trajectory shown in Fig. 11 demonstrates that the ZMP is always kept in the foot support area. 3-D simulations are shown in Fig. 12. The 3-D simulation gave five robot postures for the humanoid robot during walking.

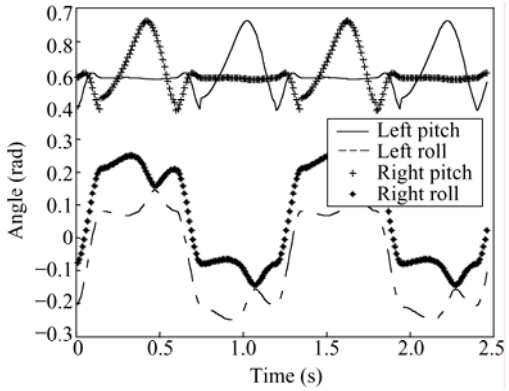

Fig. 7 Four ankle angle trajectories, two DOFs for each ankle joint

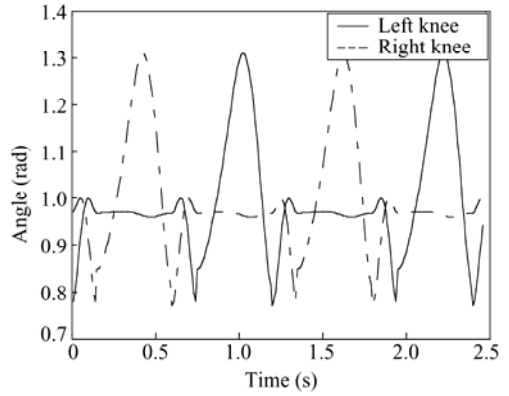

Fig. 8 Two knee angle trajectories, one DOF for each knee joint

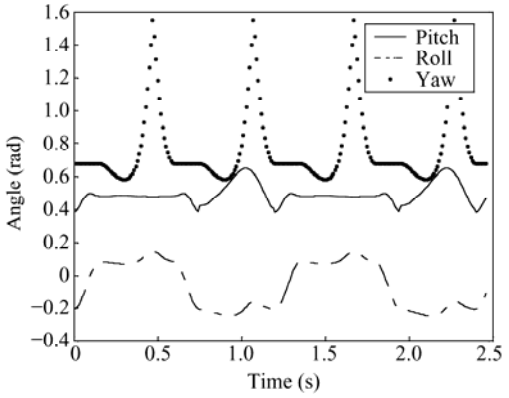

Fig. 9 Three left hip angle trajectories

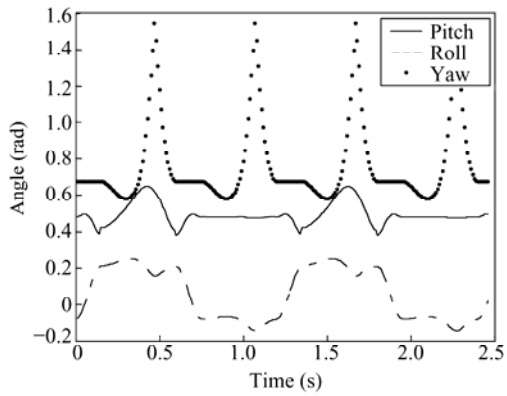

Fig. 10 Three right hip angle trajectories

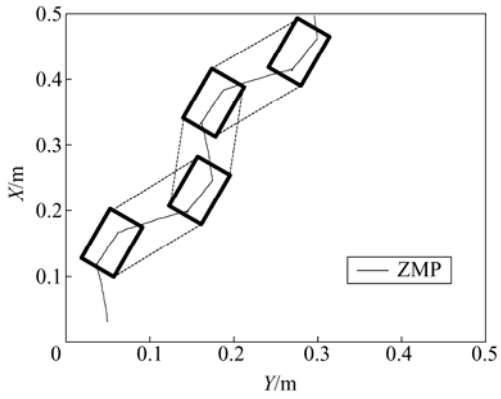

Fig. 11 ZMP trajectory

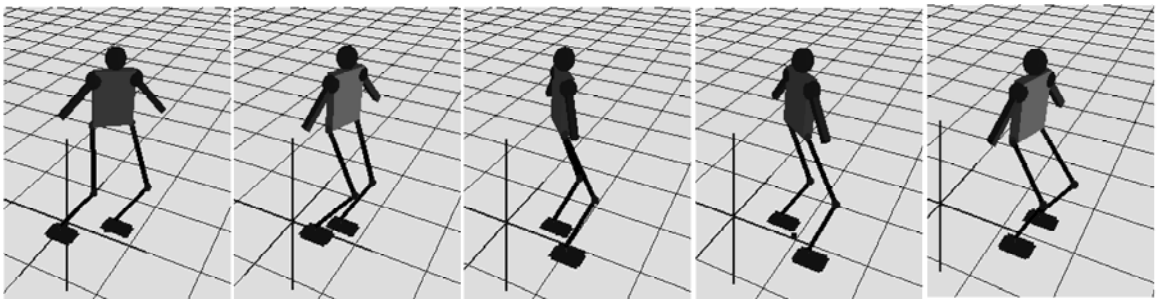

Fig. 12 3-D simulation of humanoid walking

6 Conclusions and Future Work

The planning of 3-D humanoid walking has been extensively studied. Most plans have only considered the robot movements in one plane or in two independent planes. Our proposed walking planning method identified the humanoid 3-D kinematic constraints, which allows precise conversion from the Cartesian space to the joint space. The simulation software calculates the reference trajectories of the 12 DOFs to control the robot. The robot balance is ensured by controlling the key parameters (L_p) of pelvis trajectory. The final walking gait given in this paper is not yet optimal. A trial-error procedure is needed to keep the robot from falling down and the energy consumption and ZMP error are not taken into account when planning the humanoid walking gait. In our present work[15], GAs and neural networks have been used to generate a near-optimal walking gait which minimizes the energy consumption and the ZMP error.

Humanoid robots have remarkable flexibility to adapt to complex environments compared with wheeled robots. Currently, the humanoid robots are able to realize many kinds of motion, such as walking[14], turning[16], and kicking[17]. Intelligent techniques will be integrated into humanoid robots in our future research. With this learning capability, the robot will be able to wisely combine different motions to realize more complex motion and more human-like behavior.

References

[1] Kitano H, Asada M**.** RoboCup humanoid challenge: That's one small step for a robot, one giant leap for mankind. In: Proceeding IEEE/RSJ International Conference on Intelligent Robots and Systems. 1998, **1**: 419-424.

[2] Vukobratovic M, Borovac M, Surla B, Stokic D. Biped Locomotion: Dynamics, Stability, Control and Application. Berlin-Heidelberg: Springer-Verlag, 1990.

[3] Shih C L. Gait synthesis for a biped robot. *Robotica*, 1997, **15**: 599-607.

[4] Shih C L. Ascending and descending stairs for a biped robot. *IEEE. Trans. On Systems, Man, and Cybernetics—Part A*: *Systems and Humans*, 1999, **29**: 255-268.

[5] Miyazaki F, Arimoto S. A control theoretical study on dynamical biped locomotion. *Journal of Dynamic Systems, Measurement, and Control*, 1980, **102**: 233-239.

[6] Chevallereau C, Aoustin Y. Optimal reference trajectories for walking and running of a biped robot. *Robotica*, 2001, **19**: 557-569.

[7] Furusho J, Sano A. Sensor-based control of a nine-link biped. *Int. Journal of Robotics Research*, 1990, **9**(2): 83-98.

[8] Mita T, Yamaguchi T, Kashiwase T, Kawase T. Realization of a high speed biped using modern control theory. *Int. Journal of Control*, 1984, **40**: 107-119.

[9] Miura H, Shimoyama I. Dynamic walk of a biped. *Int. Journal of Robotics Research*, 1984, **3**(2): 60-74.

[10] Zheng Y, Shen J. Gait synthesis for the SD-2 biped robot to climb sloping surface. *IEEE, Trans. Robotics, and Automation*, 1990, **6**(1): 86-96.

[11] Huang Q, Yokoi K, Kajita S, Kaneko K, Arai H, Koyachi N, Tanie K. Planning walking patterns for a biped robot. *IEEE Trans. Robot. Automat*., 2001, **17**: 280-289.

[12] Mitobe K, Moriand N, Nasu Y, Adachi N. Control of a biped walking robot during the double support phase. *Autonomous Robots*, 1997, **4**(3): 287-296.

[13] Kuffner Jr J J, Nishiwaki K, Kagami S, Inaba M, Inoue H. Footstep planning among obstacles for biped robots Intelligent Robots and Systems. In: Proceedings of IEEE/RSJ International Conference on Intelligent Robots and Systems, 2001, **1**: 500-505.

[14] Tang Z, Zhou C, Sun Z. Gait planning for soccer playing humanoid robots. Lectures Notes in Control and Information Sciences. Berlin-Heidelberg: Springer-Verlag, 2004, **299**: 241-262.

[15] Zhou C, Yue P K. Robo-Erectus: A low cost autonomous humanoid soccer robot. *Advanced Robotics*, 2004, **18**(7): 717-720.

[16] Tang Z, Zhou Changjiu, Sun Zengqi. Turning gait planning for a humanoid robot. In: Proceedings of DCDIS 4th International Conference on Engineering Applications and Computational Algorithms. Guelph, Ontario, Canada, 2005.

[17] Tang Z, Zhou C, Sun Z. Balance of penalty kicking for a biped robot. In: IEEE Int. Conf. Robotics and Automation and Mechatronics. Singapore, 2004: 336-340.

Wu Jianping Elected Chairman of APAN

Tsinghua Professor Wu Jianping, recently elected Chairman of the Asia-Pacific Advanced Network (APAN), officially assumed his new post on August 31, 2007. This is the first time a Chinese scientist has become chairman of an international internet academic organization.

APAN, a non-profit international consortium established on June 3, 1997, was designed and created as a high-performance network for research and development of advanced next generation applications and services. APAN provides an advanced networking environment for the research and education community in the Asia-Pacific region and promotes global collaboration.

(From http://news.tsinghua.edu.cn，2007-09-03)